



Assessment of Geosynthetic Materials for Tunnel Drains: Laboratory Tests and Image Analyses

Youngseok Jo^{1a}, Wonjun Cha^{2b}, Wan-Kyu Yoo^{3c}, and Bumjoo Kim^{4d}

^aDept. of Civil and Environmental Engineering, University of California at Berkeley, Berkeley 94720 CA, United States

^bDept. of Civil Engineering, University of Birmingham, Edgbaston Birmingham B15 2TT, United Kingdom

^cMember, Geotechnical Department, Korea Institute of Civil Engineering and Building Technology, Goyang 10223, Korea

^dMember, Dept. of Civil and Environmental Engineering, Dongguk University, Seoul 04620, Korea

ARTICLE HISTORY

Received 11 August 2023
Revised 13 May 2024
Accepted 29 May 2024
Published Online 5 August 2024

KEYWORDS

Tunnel drainage systems
Geosynthetic materials
Discharge capacity
Laboratory test
Secondary scanning microscopy (SEM)
Energy-dispersive X-ray spectrometry (EDS)
Calcium carbonate (CaCO₃)

ABSTRACT

Tunnel drainage systems are crucial design factors in tunnels because the accumulation of groundwater at the back of linings can affect tunnel safety. Geotextiles are used to facilitate the dissipation of pore-water pressure. However, chemical agents in the water can lead to clogging as tunnels age. In this study, laboratory tests and image analysis, namely Secondary Scanning Microscopy (SEM) and Energy-dispersive X-ray Spectrometry (EDS), were conducted to assess the drain performance of five geosynthetic materials: four geocomposites and one three-layered Non-Woven Needle-Punched (NWNP) geotextile. Calcium carbonate (CaCO₃) in liquids affects the discharge capacity of drains, and this capacity decreases with increasing confining pressure. NWNP geotextile is the most vulnerable to confining pressure as it lacks a core. The reason behind the significant decrease in the discharge capacity of NWNP geotextile is clarified based on the SEM analysis. EDS analysis investigated the major composition of the clogged materials, revealing that the primary components are carbon, oxygen, and calcium. Advanced imaging techniques can be utilized to gain a deeper understanding of the underlying mechanisms. The results of this study can aid in the design and maintenance of engineering systems, especially tunnel drainage systems, that incorporate geosynthetic materials.

1. Introduction

As tunnels are typically constructed deep underground and recently below the groundwater table, groundwater management during operation is crucial for tunnel owners. Water infiltration is the most common cause of deterioration of tunnel structures (FHWA, 2005). Since the early 1970s, geosynthetic materials have been used to facilitate the dissipation of pore-water pressure originating from water infiltration on the back of tunnels in South Korea, and their usage as tunnel drains has increased, especially in New Austrian Tunneling Method (NATM) tunnels. However, numerous previously-constructed tunnels in South Korea are aging and being affected by the infiltration of groundwater. In particular, for concrete-lined tunnels, leakage of groundwater can develop as the performance of concrete lining waterproofing is reduced due to chemical agents in the groundwater. Woo and Yoo (2004) examined the drainage systems of Seoul Metropolitan

Subway tunnels and reported that white precipitates found in the drainage systems reduce drain performance and contain a large amount of calcium oxide (CaO) primarily from the grouts used for tunnel reinforcement (Fig. S1 and S2). Chun et al. (2011) examined the drainage system in the Namsan tunnel, Seoul, in September 2010, and observed white precipitates in the drain system and cavities around the tunnel, as shown in Fig. S3. Additionally, in tunnels with drainage systems, the build-up of transported material and compression of filters, especially geotextiles, due to the weight of the tunnels may hinder seepage into the tunnels. Reduction in drainage capacity as a result of fine-particle migration, clogging, and accumulation into seepage routes in the primary lining or the filter could lead to the development of pore-water pressure on the tunnel lining, thereby rendering the tunnel unstable (Shin et al., 2005).

In South Korea, for efficient dissipation of groundwater infiltration, KR (2017), an organization responsible for tunnel-

CORRESPONDENCE Bumjoo Kim ✉ bkim1@dongguk.edu ☒ Dept. of Civil and Environmental Engineering, Dongguk University, Seoul 04620, Korea

© 2024 Korean Society of Civil Engineers

related criteria, reported that non-woven geotextiles should be installed between tunnel linings and shotcrete to secure sufficient discharge capacity (i.e., to reduce pore-water pressure sufficiently). They recommended examining the clogging potential of drains and, if necessary, evaluating the thickness of non-woven geotextiles to increase them appropriately or installing additional materials (e.g., drain boards) to reduce the pore-water pressure on the backs of tunnels. In accordance with these criteria, Jang et al. (2015) performed laboratory tests to analyze the discharge capacities of non-woven geotextiles comprising a few layers (ranging from one layer to three layers) depending on different confining pressures. They reported that non-woven geotextiles have a high clogging potential and weak resistance against confining pressures.

In this study, discharge capacity tests were conducted to assess the performance of geosynthetic materials for tunnel drains, possibly to replace the existing tunnel drain (i.e., Non-woven Needle-Punched geotextile (*hereafter* NWNP), for the tunnel design and maintenance. The performance of NWNP, used as the tunnel drain in South Korea, was compared with that of four geocomposites originally designed for ground improvement (i.e., Prefabricated Vertical Drains, PVDs). The investigation particularly focused on the clogging of drains due to calcium carbonate (CaCO_3) precipitation. The effects of both the presence of CaCO_3 in liquids and confining pressure were analyzed based on laboratory tests. Furthermore, changes in the cross-sectional area of geosynthetic materials were investigated using discharge capacities determined from the tests. Additionally, Scanning Electron Microscopy (SEM) and Energy-Dispersive X-ray Spectrometry (EDS) were conducted to apprehend the clogged materials between geosynthetic drain fabrics. Based on these overall results, the performance of five geosynthetic tunnel drains was evaluated.

2. Materials and Methods

2.1 Geosynthetics for Drain

The materials utilized in this study consisted of various types of geocomposites consisting of a polymer core encased by a geotextile,

commonly known as geotextile-polymer core composites. The polymer core was engineered to facilitate the efficient flow of a substantial volume of liquid through its structure, thereby functioning as a drainage core. Meanwhile, the geotextile served to shield the core and served as a filter and separator on both sides.






Four geocomposites were tested, depending on the types of drainage core and geotextile filter, as presented in Table 1. They possessed three shapes (namely, harmonica shape for GC-1 & 2, castle shape for GC-3, and retiform shape for GC-4) and two different filter types (namely, thermal heat-bonded type for GC-1, 2, 3 and needle-punched type for GC-4). The detailed information, including cross-sectional area, hydraulic conductivity, and core & filter thickness, is presented in Table 1, as well as the results of pore distribution tests (i.e., Apparent Opening Size (AOS) and Effective Opening Size (EOS)).

In South Korea, NWNP geotextiles have primarily been used for geosynthetic drains in the design and construction of tunnels. An example of the quality standard for tunnel drain materials suggested by the Korea Expressway Corporation is presented in Table S1 (KEC, 2010). As described in the Introduction, geotextiles with varying thicknesses, ranging from one to three layers, can be used for tunnel drains. In this study, three-layered NWNP geotextiles were used in the laboratory tests for comparison with the geocomposites in terms of discharge capacity, although one-layered NWNP geotextile satisfies the quality standard of geosynthetic materials for the tunnel drain (Table S1). This is because one-layered NWNP geotextile is considered significantly weaker in confining pressure compared to three-layered geotextiles and geocomposites with cores.

2.2 Apparatus for Laboratory Tests

The laboratory testing apparatus was adapted from the Delft test apparatus, which was originally developed for the prefabricated vertical drain discharge test by Oostveen and Troost (1990). The geosynthetic materials (specifically geocomposites) employed in this study closely resemble PVD (prefabricated vertical drain) materials, featuring a geotextile filter and core structure. The

Table 1. Specifications Related to Geosynthetic Materials Used in Laboratory Tests

Geosynthetic materials	GC-1	GC-2	GC-3	GC-4	NWNP geotextile
Cross section					
Cross-sectional area, A (cm ²)	4.0	11.0	3.0	4.5	8.2
Permeability (cm/s)	16.56	3.44	24.00	13.81	0.29
Core shape	Harmonica		Castle	Retiform	-
Core thickness (mm)	4.0	11.0	3.0	4.5	8.2
Filter type	Thermal Heat Bonded			Needle punched	Non-woven needle punched
Filter thickness (mm)	0.2	0.6	0.35	1.0	8.2
AOS (mm)	0.228	0.148	0.247	0.103	-
FOS (mm)	0.191	0.156	0.208	0.108	-

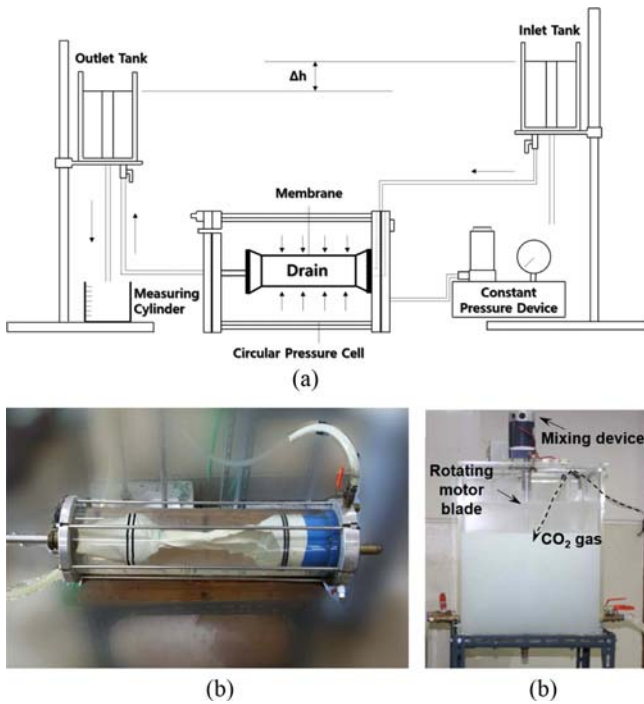


Fig. 1. Discharge Capacity Test Apparatus: (a) Schematic Layout, (b) Cylindrical Chamber and Sample, (c) CaCO₃ Generation Device

apparatus used herein consists of a cylindrical chamber (i.e., circular pressure cell) with a diameter of 20 cm and height of 55 cm, a constant pressure device, and a measuring cylinder. The three-layered NWNP geotextile was also used in the tests in the same manner. The graphical layout of the apparatus is shown in Fig. 1(a).

Geosynthetic materials, measuring 10 cm in width and 43 cm in length, were affixed to the top and bottom pedestals within the chamber and enveloped with a membrane to isolate the sample from the water in the chamber. To enable water to enter the drainage core through the geotextile filter, one end of the sample was sealed using the geotextile filter. Table S2 shows filters that are the ends of the samples after the tests, and the red-dotted line indicates the location where a clamp was installed to fix the filter. Following saturation of the sample, the chamber filled with distilled water was positioned horizontally (see Fig. 1(b)), and three different cell pressures (50, 200, and 400 kPa) were applied for each test. The maximum cell pressure of 400 kPa was chosen to align with typical pressures experienced by tunnel linings in South Korea, representing the range of design considerations. The hydraulic gradient (i) applied to the system was 0.5, falling within the recommended range specified by ASTM D4716-08 (2013) and ISO 12958-2 (2020) standards. The test was operated over 6 hours at each cell pressure. ASTM D4716 and ISO 12958 are standards related to testing methods for determining the flow rate per unit width and hydraulic transmissivity of a geosynthetic using a constant head and the water flow capacity of geotextiles, respectively. The water level of an inlet tank in Fig. 1(a) was constantly maintained during the tests. Additionally, both fresh

Table 2. The Condition of Discharge Capacity Test

Geosynthetic materials	Confining pressure (kPa)	Hydraulic gradient (i)	Initial discharge capacity (cm ² /s)
GC-1	50, 200, 400	0.5	6.62
GC-2			13.79
GC-3			7.80
GC-4			6.21
NWNP geotextile			0.24

distilled water and CaCO₃ liquid were used as permeating water for each test.

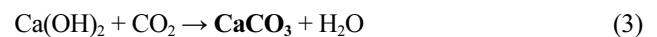
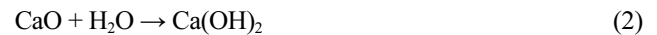
The discharge capacity under the designed confining pressure was then obtained by monitoring water flow and calculated using the Eq. (1).

$$q_w = Q/i, \quad (1)$$

where q_w is the discharge capacity, Q is the water flow via the geosynthetic materials, and i is the hydraulic gradient (0.5 in this study). Based on Eq. (1), the initial discharge capacities for each geosynthetic material (i.e., GC-1, 2, 3, 4, and NWNP geotextile) were determined to be 6.62, 13.79, 7.80, 6.21, and 0.24 cm²/s, respectively (Table 2).

2.3 Preparation of Calcium Carbonate Water

Calcium carbonate (CaCO₃) precipitation is identified as a significant cause of drain clogging in underground tunnels (Woo and Yoo, 2004; Dietzel et al., 2008; KICT, 2009). Groundwater flowing through shotcrete on tunnel walls can dissolve the concrete, shotcrete, and grout used in surrounding soil or rock fractures for reinforcement, due to the interconnected pores and microcracks present in these materials (Gascoyne, 2002). Calcium hydroxide (Ca(OH)₂) leachates from concrete, resulting from the reaction of calcium oxide (CaO) (i.e., lime) in cement with groundwater, may further react with carbon dioxide (CO₂) primarily emitted from vehicles, leading to the formation of CaCO₃ (Eq. (3)).



In this study, distilled water with CaCO₃ was prepared to analyze the effect of the presence of CaCO₃ in groundwater on geosynthetic filters and to assess the performance of tunnel drains (i.e., four geocomposites and an NWNP geotextile). Fig. 1(c) shows the CaCO₃ generation device (i.e., inlet tank in Fig. 1(a)). Distilled water (H₂O) and CaO, with a mass equivalent to 0.17% of the water by weight, were combined in a bath and allowed to mix for 24 hours to produce Ca(OH)₂. Subsequently, the liquid containing dissolved Ca(OH)₂ was transferred to an inlet tank measuring 42 cm in width, 42 cm in length, and 52 cm in height, equipped with a mixing device. CO₂ gas was then introduced into the inlet tank to induce the formation of CaCO₃, while a rotating motor blade on the mixing device agitated the liquid for an additional 24 hours. The precipitation of CaCO₃ in liquids is known to be influenced

by water temperature, with the solubility of CaCO_3 decreasing as water temperature increases (Siegel and Reams, 1966). Therefore, the entire experimental procedure was conducted at a constant temperature of 15°C to ensure consistent and controlled conditions for the study.

2.4 Scanning Electron Microscope and Energy Dispersive X-ray Spectrometer

After the laboratory tests, clogged materials on the surface and inside the filters were observed using SEM. As the geosynthetic and clogged materials are not conductive, they were placed on carbon tape and coated with platinum to convert them into conductors. In general, the Secondary Electron Image (SEI) method is used to scan specimens. However, in this study, another method using Backscattered Electron (BSE) was used to observe the geosynthetic and clogged materials; this method can distinguish the materials based on information related to the material composition. Additionally, an EDS mounted on a SEM device was used to investigate the characteristics of clogged materials. The JSM-7800F Schottky Field Emission scanning electron microscope was used for the laboratory tests.

3. Results and Discussion

3.1 Effect of the Presence of CaCO_3 in Liquids

Figure 2 shows the changes in discharge capacity over the elapsed time under three confining pressure levels (50, 200, and 400 kPa) for the geosynthetic materials, with and without the presence of CaCO_3 in the liquid. Evidently, the presence of CaCO_3 in liquids affects the discharge capacity of geosynthetic materials. Overall, the discharge capacity of non- CaCO_3 liquid was larger than that of CaCO_3 liquid, implying that the presence of CaCO_3 affects the discharge capacity of tunnel drains.

The level of decreased discharge capacity for each geosynthetic material under different confining pressures was expressed as the ratio of discharge capacities with and without CaCO_3 ($q_{no, \text{CaCO}_3}/q_{with, \text{CaCO}_3}$). The values for each material ranged as follows: a) The ratio of GC-1 ranged from 0.39 to 0.52 (0.45 on average); b) The ratio of GC-2 ranged from 0.13 to 0.35 (0.21 on average); c) The ratio of GC-3 ranged from 0.49 to 0.71 (0.63 on average); d) The ratio of GC-4 ranged from 0.48 to 0.57 (0.52 on average); e) The ratio of NWNP geotextile ranged from 0.57 to 0.66 (0.61 on average).

Based on these results, GC-3 showed the best performance as a tunnel drain among the geocomposites. In addition, the AOS and FOS of GC-3 were determined to be the highest as shown in Table 1. It indicated that the permeability of the GC-3 is originally high and good. The discharge capacities of NWNP geotextile varied in a narrow range. In particular, there was no significant difference in confining pressure 50 and 200 kPa, because the NWNP geotextile has no cores which can protect the filter against confining pressures. The mean ratio of discharge capacity for NWNP geotextile was higher than that of GC-1, 2, and 4 because the discharge capacity of NWNP geotextile without CaCO_3 in

the liquid was initially very low. The initial discharge capacities for each geosynthetic material are listed in Table 2.

3.2 Effect of the Confining Pressures

After the confining pressure began acting on the geosynthetic materials, the discharge capacities of GC-2 and NWNP geotextile decreased significantly (Figs. 2(d) – 2(f) and Figs. 2(m) – 2(o)). This was caused by the following two reasons: a) As shown in Table 1, the core gap of GC-2 was larger than that of other geocomposites (i.e., GC-1, 3, and 4). This enabled the filter to reach between the gaps of the core after the confining pressure began acting and disrupted the flow. b) Since the NWNP geotextile has no cores, it was vulnerable to confining pressures. In particular, the discharge capacity of the NWNP geotextile was the lowest among the tested geosynthetic materials.

Figure 3 shows the changes in the determined discharge capacities depending on confining pressures while the CaCO_3 liquid was used for the laboratory tests. Evidently, the discharge capacities of geosynthetic materials decreased as the confining pressures increased. GC-3 showed the best performance and was least affected by confining pressures. The discharge capacity of GC-2 was the lowest, while the NWNP geotextile was identified as the most vulnerable to confining pressure. In particular, the NWNP geotextile was identified as the most vulnerable to confining pressure because it has no core in contrast with other geosynthetic materials.

3.3 Changes in the Effective Pore-Area of Geosynthetic Materials

A sufficient cross-sectional area should be secured in order to drain groundwater for tunnel drainage systems. In this study, the changes in the cross-sectional area were analyzed based on the hypothesis that the area where fluid can flow is reduced by CaCO_3 precipitation. Fig. 4 shows the changes in the cross-sectional area with confining pressures when the CaCO_3 liquid permeated the geosynthetic materials. The cross-sectional area was calculated using Eq. (3), where K is the permeability of geosynthetic materials, which was determined based on the distilled water. Therefore, in this section, the variation of the cross-sectional area was analyzed based on the hypothesis that the changes in the discharge capacity are only related to the decrease in the cross-sectional area of geosynthetic materials when their permeability is fixed.

$$Q = K \times i \times A, \quad (4)$$

where Q is the flow rate, K is the permeability of geosynthetic materials, i is the hydraulic gradient, and A is the cross-sectional area of geosynthetic materials.

The tests revealed that the cross-sectional area for each geosynthetic material drastically decreased (Fig. 4(a)) due to the effect of confining pressure. The area reduction of GC-2 and NWNP geotextile was larger than that of other materials (i.e., GC1, 3, and 4), and the reason for this has been described in Section 3.1. From the zoomed-in image in the dotted box in Fig. 4(a), the changes in the cross-sectional area of geosynthetic materials with confining

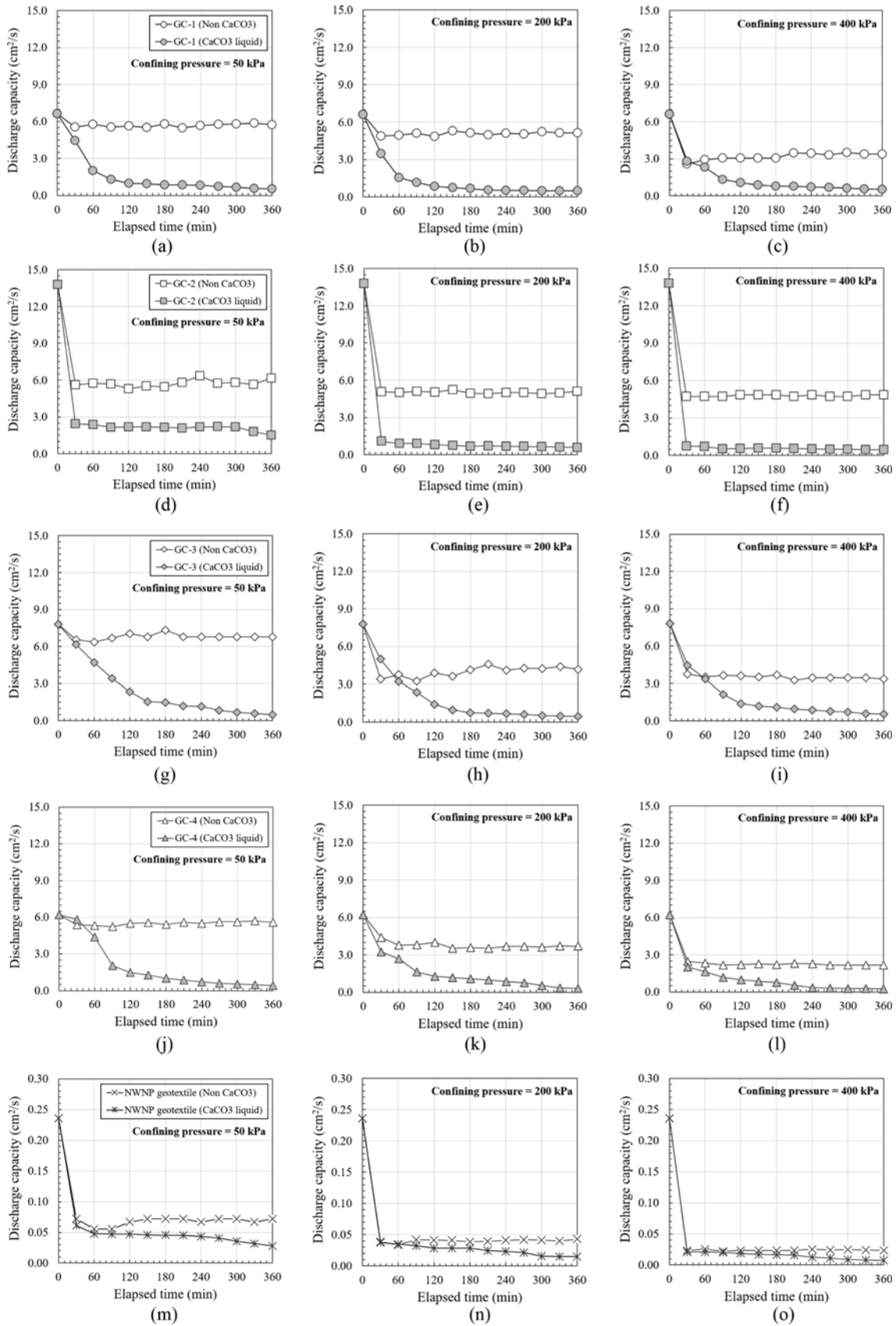


Fig. 2. Changes in the Discharge Capacity over Elapsed Time Depending on the Presence of CaCO₃ in Liquids: (a – c) GC-1, (d – f) GC-2, (g – i) GC-3, (j – l) GC-4, (m – o) NWNP Geotextile

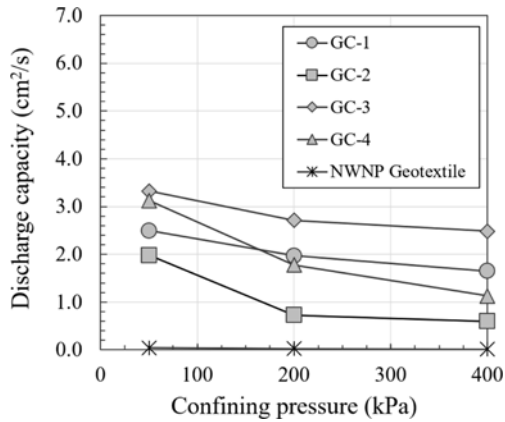


Fig. 3. Changes in the Discharge Capacities Depending on Confining Pressures When the CaCO₃ Liquid Was Used for the Laboratory Tests

pressures are shown in Fig. 4(b). Overall, changes in the cross-sectional area of GC-3 were the smallest, and the sudden change related to GC-3 in Fig. 4(b) did not appear in the confining pressure range between 50 and 400 kPa. This implies that among the tested geosynthetic materials, GC-3 was the most durable against clogging and confining pressure and could maintain the discharge

capacity under those conditions. The cross-sectional areas of GC-2 and NWNP geotextile were the lowest as the confining pressure reached 400 kPa.

3.4 Investigation by SEM and EDS

3.4.1 Identification of Clogged Materials

Figure 5 shows the SEM results for the clogged materials in the texture of the NWNP geotextile. The views of lightly and heavily clogged areas are shown in Figs. 5(a) and 5(b), respectively. Fig. 5(c) shows the cross-sectional view; evidently, clogged materials filled the spaces between the fibers of the NWNP geotextile. Using these figures, the reasons behind the drastic decrease in discharge capacity for NWNP geotextile can be explained as follows: a) The pores and paths where the fluid can flow disappeared due to the clogged materials. b) As the NWNP geotextile did not have skeletons that could support against confining pressure, it became more vulnerable to confining pressure compared to geocomposites. c) The combination of the above conditions (i.e., the clogged materials and no skeleton structure) accelerated the drastic reduction of discharge capacity. EDS was conducted to investigate the composition of the clogged materials, and the results are shown in Fig. 6. The major composition of the

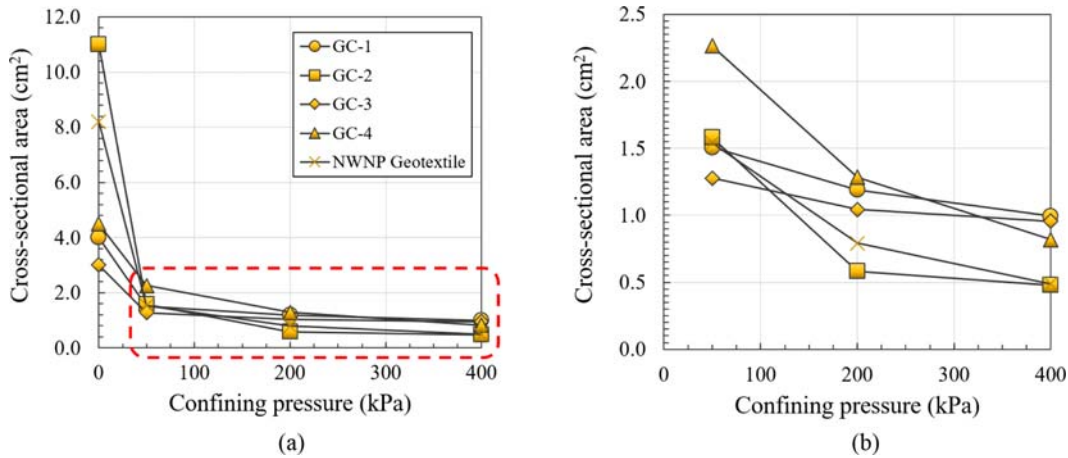


Fig. 4. Changes in the Cross-Sectional Area of Geosynthetic Materials Depending on Confining Pressure While CaCO₃ Liquid Was Injected: (a) from the Beginning to the End of the Laboratory Tests, (b) Zoom-in the Dotted Box in Fig. 4(a)

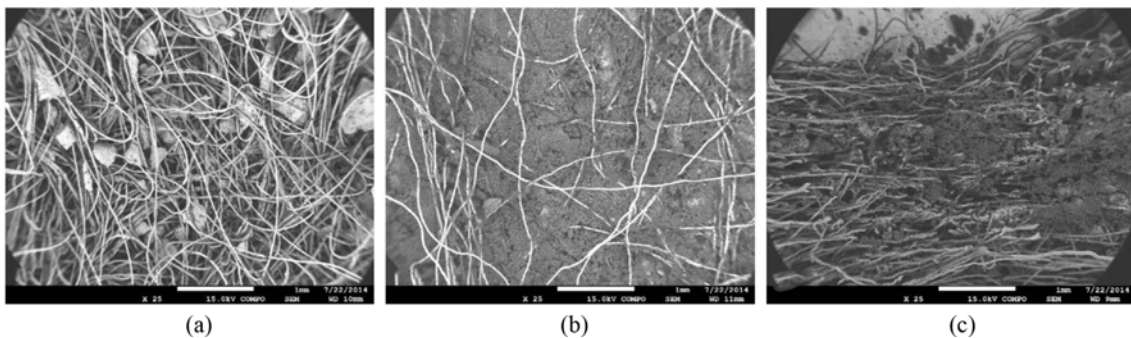


Fig. 5. SEM Results for the Clogged NWNP Geotextile: (a) Plan View of a Lightly Clogged Area (×25), (b) Plan View of a Heavily Clogged Area (×25), (c) Cross-Sectional View (×25)

clogged materials was found to be carbon (C), oxygen (O), and calcium (Ca).

3.4.2 Pore-Scale Analysis by Image Processing Techniques

In this section, the asymptotic (i.e., minimum or terminal) permeability for fully clogged geocomposites was analyzed based on SEM images. The clogging of geosynthetic materials has a critical impact on the permeability of the entire tunnel stability. In order to properly design and maintain tunnel systems, accurately estimating the asymptotic permeability for a given system is essential. This is particularly important in the case of drainage systems, as clogging can occur over time due to a variety of factors, such as the accumulation of sediment or the growth of microorganisms.

In this study, multiple SEM images were utilized to gain a deeper understanding of the pore-scale behavior of CaCO₃-covered geocomposites. The SEM analysis revealed that the CaCO₃ was deposited between the geocomposite fibers (Fig. S4), thereby reducing the porous zone and leading to a decrease in permeability. To further investigate this phenomenon, different image processing techniques were employed to analyze the SEM images. These

techniques included denoising, trained statistical pixel classification, segmentation and labeling, and pore size distribution analysis. To

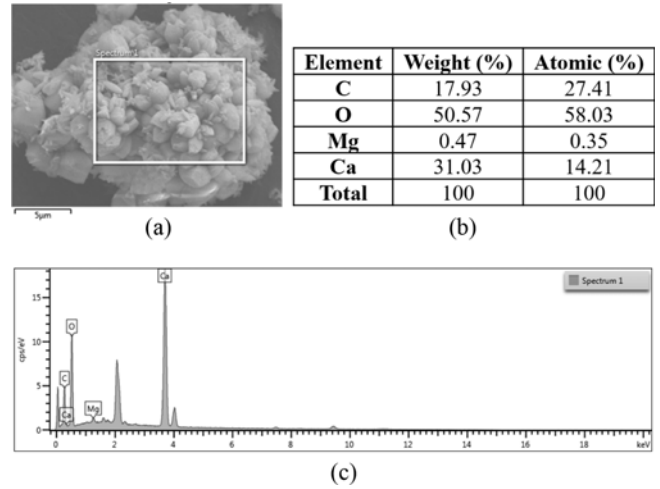


Fig. 6. EDS Results for the Clogged Material: (a) Precipitated Material Sampled for EDS Analysis, (b) Results of Quantitative Analysis, (c) EDS Graph for the Sampling Materials

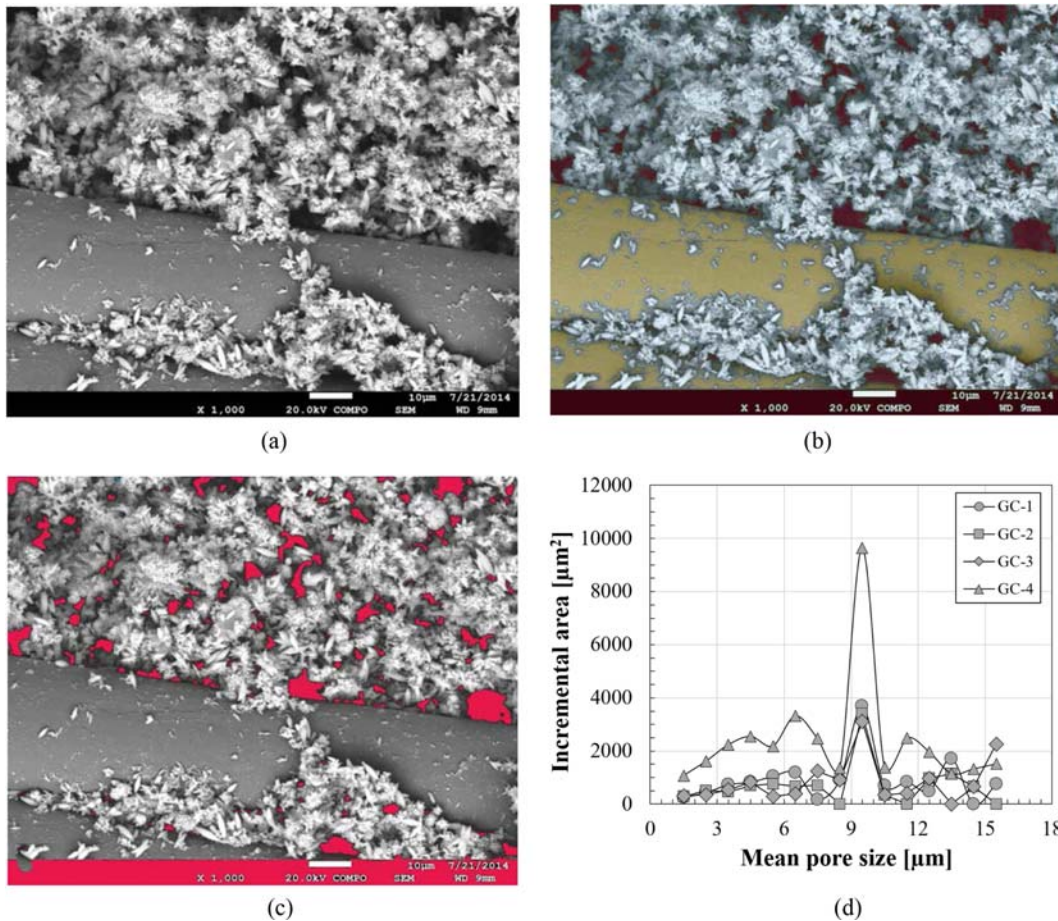


Fig. 7. Pore-Scale Analysis for the Clogged Geocomposite (x1000): (a) An Original SEM Image of Fully Clogged Geocomposite (GC-1 in Table 1), (b) Trained Pixel Classification for Three Component System with Geocomposite Fiber, CaCO₃, and Pore (Yellow: Geocomposite Fiber, Blue: CaCO₃, Red: Pore), (c) Pore Segmentation Overlaps with a Raw SEM Image, (d) 2D Equivalent Circular Pore Size Distribution for Four Types of Clogged Geocomposite

obtain accurate and reliable results, a combination of Ilastik, ImageJ, and Matlab software was used for image processing. The results of the analyses are presented in Fig. 7, which includes a variety of graphical representations of the pore size distribution and permeability of fully clogged geocomposites. The estimated mean pore diameter for all cases was found to be 9.5 μm , indicating that the opening size of the geocomposites does not have a significant effect on the asymptotic mean pore diameter for this system.

Furthermore, the analysis yielded an estimated asymptotic permeability of $4.5 \times 10^{-10} \text{ m}^2$ using the Kozeny-Carman equation. The estimated value is smaller than the permeability measured after 6 hours (i.e., 360 mins) of testing. When the pore size in the layers of a geocomposite becomes smaller than the core due to clogging, the core may begin to act as a bypass. This can significantly impact the system's performance, necessitating strategies to minimize clogging and ensure long-term performance.

4. Conclusions

An assessment of geosynthetic materials aimed at replacing conventionally used tunnel drains in Korea was performed in this study. A series of discharge capacity tests was conducted using five geosynthetic materials (four geocomposites and one three-layered NWNP geotextile). The effect of the presence of CaCO_3 in liquid and that of confining pressure was analyzed with regard to the discharge capacity of geosynthetic materials. Next, changes in the effective pore area were investigated based on the discharge capacities for each material under different confining pressures. Additionally, SEM and EDS analyses were performed to examine the clogged materials between geosynthetic drain fabrics. The following conclusions were drawn from the analyzed results. The presence of CaCO_3 in liquids affects the discharge capacity of geosynthetic materials. Overall, the discharge capacity of non- CaCO_3 liquid was larger than that of CaCO_3 liquid, which implies that the presence of CaCO_3 affects the discharge capacity of tunnel drains. Subsequently, the level of the decreased discharge capacity for each geosynthetic material under different confining pressures was expressed as the ratio of discharge capacities with and without CaCO_3 (i.e., q_{ns} , non- $\text{CaCO}_3/q_{\text{w}}$, CaCO_3). Based on each ratio for different geosynthetic materials, GC-3 exhibited the best performance as a tunnel drain.

Regarding the confining pressure, the decrease in the discharge capacities of GC-2 and NWNP geotextile was the largest for the following reasons: a) The core gap of GC-2 was larger than that of other geocomposites (i.e., GC-1, 3, and 4), and the filter of GC-2 easily reached between the gaps of the core; b) As the NWNP geotextile had no cores, it was vulnerable to confining pressure. In particular, the discharge capacity of the NWNP geotextile was the lowest among the tested geosynthetic materials. Additionally, GC-3 exhibited the best performance as a tunnel drain because it was least affected by confining pressures. At the beginning of the tests, the cross-sectional area for each geosynthetic material significantly decreased due to the effect of confining

pressure. Overall, changes in the cross-sectional area of GC-3 were the smallest, and the sudden change related to GC-3 did not appear for the entire range of confining pressure considered. This implies that GC-3 has the ability to maintain the discharge capacity against clogging by CaCO_3 precipitation and confining pressure.

Based on the SEM and EDS analyses, the discharge capacity of the NWNP geotextile decreased significantly because the pores and paths where the fluid could flow disappeared owing to the clogged materials. Moreover, the NWNP geotextile was more vulnerable to confining pressure compared with geocomposites owing to the lack of a supporting skeleton structure. Further, the major components of the clogged materials were found to be carbon, oxygen, and calcium based on the EDS analysis.

Thus, the obtained results suggest that the clogging of geocomposites can have a significant impact on permeability and that advanced imaging techniques can be used to gain a deeper understanding of the underlying mechanisms. The results of this study can aid in the design and maintenance of engineering systems, particularly tunnel drainage systems, that incorporate geosynthetic materials.

Acknowledgments

This work was supported by the Dongguk University Research Fund of 2023.

ORCID

Youngseok Jo  <https://orcid.org/0000-0003-3162-7562>
 Wonjun Cha  <https://orcid.org/0000-0002-3897-2863>
 Wan-Kyu Yoo  <https://orcid.org/0000-0001-9344-656X>
 Bumjoo Kim  <https://orcid.org/0000-0003-2955-793X>

References

- ASTM D4716-08 (2013) Standard test method for determining the (In-plane) flow rate per unit width and hydraulic transmissivity of a geosynthetic using a constant head. *ASTM International*, West Conshohocken, PA, DOI: [10.1520/D4716-08](https://doi.org/10.1520/D4716-08)
- Chun BS, Jang YS, Kim B (2011) Final report: Development of technology for improving the tunnel drainage system in old tunnels. Seoul Metropolitan Government, Republic of Korea (in Korean)
- Dietzel M, Rinder T, Leis A, Reichl P, Sellner P, Draschitz C, Plank G, Klammer D, Schofer H (2008) Koralm tunnel as a case study for sinter formation in drainage systems—precipitation mechanisms and retaliatory action. *Geomechanik und Tunnelbau* 1(4):271-278, DOI: [10.1002/geot.200800024](https://doi.org/10.1002/geot.200800024)
- FHWA (2005) Highway and rail transit tunnel inspection manual. FHWA-NHI-09e010. Federal Highway Administration, US Department of Transportation, Washington, D.C.
- Gascoyne M (2002) Influence of grout and cement on groundwater composition. Possiva Working Report, 7: 44, Helsinki, Finland
- ISO 12958-2 (2020) Geotextile and geotextile related products - determination of water flow capacity in their plane, *International Organisation for Standardisation*, CH-1211, Geneva

- Jang YS, Kim B, Lee JW (2015) Evaluation of discharge capacity of geosynthetic drains for potential use in tunnels. *Geotextiles and Geomembranes* 43(3):228-239, DOI: [10.1016/j.geotexmem.2015.03.001](https://doi.org/10.1016/j.geotexmem.2015.03.001)
- KEC (2010) Quality and test standard of construction materials for express highway construction, Korea Expressway Corporation (in Korean)
- KICT (2009) Development of safety maintenance and disaster prevention technology (VI) KICT Report 2009-069. Korea Institute of Construction Technology, Kyeonggi-do, Korea, 233 (in Korean)
- KR (2017) Standard specification for tunnel design. KR C-12060_Rev.2, Korea Rail Network Authority (in Korean)
- Oostveen JP, Troost GH (1990) Discharge index tests on vertical drains. Proceedings of the Fourth International Conference on Geotextiles, Geomebranes, and Related Products: Steep slopes and walls. Embankments on soft soil. Roads and railroads. Filtration and drainage. *Erosion control, The Hague, Netherlands* 1:345-350
- Shin JH, Potts DM, Zdravkovic L (2005) The effect of pore-water pressure on NATM tunnel lining in decomposed granite soil. *Canadian Geotechnical Journal* 42(6):1585-1599, DOI: [10.1139/t05-072](https://doi.org/10.1139/t05-072)
- Siegel FR, Reams MW (1966) Temperature effect on precipitation of calcium carbonate from calcium bicarbonate solutions and its application to cavern environments. *Sedimentology* 7:241-248, DOI: [10.1111/j.1365-3091.1966.tb01597.x](https://doi.org/10.1111/j.1365-3091.1966.tb01597.x)
- Woo JT, Yoo SG (2004) A study on analysis of influx path and ingredient of sedimentation substance in tunnel drainage system. *Journal of Korean Tunnelling and Underground Space Association* 8(4):145-153 (in Korean)